

Document downloaded from:

<http://hdl.handle.net/10251/81814>

This paper must be cited as:

Salvador Rubio, FJ.; Romero Bauset, JV.; Roselló Ferragud, MD.; Jaramillo-Císcar, D. (2016). Numerical simulation of primary atomization in diesel spray at low injection pressure. *Journal of Computational and Applied Mathematics*. 291:94-102. doi:10.1016/j.cam.2015.03.044.



The final publication is available at

<http://doi.org/10.1016/j.cam.2015.03.044>

Copyright Elsevier

Additional Information

Numerical simulation of primary atomization in diesel spray at low injection pressure

F.J. Salvador^{a,*}, J.-V. Romero^b, M.-D. Roselló^b, D. Jaramillo^a

^a*CMT-Motores Térmicos,
Universitat Politècnica de València,
Camino de Vera s/n, Edificio 6D
46022, Valencia, Spain*

^b*Instituto Universitario de Matemática Multidisciplinar,
Universitat Politècnica de València,
Camino de Vera s/n, Edificio 8G, 2º
46022, Valencia, Spain*

Abstract

Atomization involves complex physical processes and gas-liquid interaction. Primary atomization on diesel spray is not well understood due to the difficulties to perform experimental measurements in the near nozzle field. Hence computational fluid dynamics (CFD) has been used as a key element to understand and improve diesel spray.

A recent new code for incompressible multiphase flow with adaptive octree mesh refinement has been used to perform simulations of atomization at low injection pressure conditions. The multiphase flow strategy to manage different flows is the volume of fluid (VOF) method. The adaptive mesh allows to locally refine the mesh at each time step where a better resolution is needed to capture important gradients instead of using a static mesh with a fixed and high number of cells which, in turns, would lead to an unaffordable computational cost. Even with this approach, the cell number is very high to achieve a Direct Numerical Simulation (DNS) at reasonable computational cost. To reduce the computational cost, an idea has been explored, the possibility of setting a maximum number of cells of the domain. Following this idea, the code has been tested with different configurations to understand their effects on numerical stability, the change in different spray parameters and the benefits achieved in terms of execution time. The outcomes have been validated against a theoretical model.

Keywords: diesel spray, atomization, Gerris, DNS, VOF

1. Introduction

Atomization process in a spray has been an important issue for researchers during last decade, due to its presence in many industrial applications. In particular, this is extremely important in

*Corresponding author: Dr. F. Javier Salvador, Telephone: 34-963879659, Fax: 34-963877659
Email addresses: fsalvado@mot.upv.es (F.J. Salvador), jvromero@imm.upv.es (J.-V. Romero),
drose11o@imm.upv.es (M.-D. Roselló), dajacis@mot.upv.es (D. Jaramillo)

4 Diesel Engines, where combustion efficiency and pollutant formation are a consequences of spray
5 atomization and fuel-air mixing process [1, 2, 3, 4, 5].

6 As a result of these studies, several tools have been developed for modeling macroscopic
7 spray behaviour [6, 7]. Nevertheless, there are still uncertainties related with internal nozzle flow
8 and its link with spray formation and primary break-up [8, 9, 10].

9 Last decades have been characterized by a continuous increase in computational resources.
10 For the study of diesel spray this increase allows to move forward to use more complex models
11 for breakup, evaporation, coalescence, turbulence, etc.

12 In terms of turbulence modelling, the classes of models from lower to higher computational
13 cost are: RANS (Reynolds averaged Navier-Stokes) [11, 12], LES (large eddy simulations) [13,
14 14] and DNS (direct numerical simulations) [15, 16, 17]. While RANS methods have been used
15 along several decades, the use of LES models is more recent and even now the computational
16 requirements for the use of DNS is still very high for study typical current conditions in diesel
17 engines.

18 However, despite all the computational difficulties some researchers [16, 17, 18] have tried to
19 use DNS approach for the study of Diesel sprays. Some basic procedures have been adopted by
20 these researchers in order to be able to perform DNS simulations in sprays, such as, decreasing
21 injection velocity and reducing the domain for studying only the first millimeters, and so, taking
22 into account only primary atomization. It is also used an Adaptative Mesh Refinement (AMR)
23 method to reduce the computational cost of simulations [17, 18]. Even with this simplifications,
24 in the present paper, the numerical cost to simulate around 8 millimeters of the spray has been
25 around 2 months running over 32 CPUs on a blade server Fujitsu BX920.

26 The aim of this paper is to study the potential of a new code [19, 20] to perform simulations
27 of primary atomization in diesel sprays with DNS approach. For this purpose the same strategy
28 used by other researchers described before [16, 17, 18] for reducing the computational time has
29 been used: Low spray velocity, small domains (just to consider only the first atomization and
30 breakup length) and the application of AMR algorithm.

31 The present paper has been split into 6 sections. In Section 2, a brief description of the
32 numerical code will be performed. After that, in Section 3, a mesh sensitivity study performed
33 over several parameters that define the mesh will be reported. In Section 4 the outcomes of the
34 computational simulations will be validated against a theoretical model available in the literature
35 (which in turns has been widely validated). After the validation, in Section 5, a study on the
36 influence that the use of periodic perturbation in the injection velocity has on the results will be
37 described. Finally, in Section 6 the main conclusions will be drawn.

38 2. Numerical Code

39 For this study, the numerical code Gerris developed by Stéphane Popinet [19, 20] has been
40 used. This code solves Navier-Stokes equations with surface tension for incompressible flow
41 (1)–(3)

$$42 \quad \rho(\partial_t \mathbf{u} + \mathbf{u} \cdot \nabla \mathbf{u}) = -\nabla p + \nabla \cdot (2\mu \mathbf{D}) + \sigma k \delta_s \mathbf{n}, \quad (1)$$

$$43 \quad \partial_t \rho + \nabla \cdot (\rho \mathbf{u}) = 0, \quad (2)$$

$$\nabla \cdot \mathbf{u} = 0, \quad (3)$$

44 where $\rho = \rho(\mathbf{x}, t)$ is the fluid density, $\mathbf{u} = (u_x, u_y, u_z)$ is the fluid velocity, p is the pressure
45 field, $\mu = \mu(\mathbf{x}, t)$ is the dynamic viscosity, \mathbf{D} is the deformation tensor, σ is the surface tension

46 coefficient, k and \mathbf{n} are the curvature and the normal vector to the interface, respectively, and δ_s is
 47 the Dirac distribution which expresses that the surface tension term is active only in the interface.

48 In the simulations whose results are presented here, diesel fuel is injected into a gas envi-
 49 ronment, thus, density and viscosity depend of the concentration of diesel, c , in the following
 50 way

$$\rho(c) = c\rho_f + (1 - c)\rho_a, \quad (4)$$

$$\mu(c) = c\mu_f + (1 - c)\mu_a, \quad (5)$$

52 where ρ_f and ρ_a are the fuel and air density, respectively, and μ_f and μ_a represent the fuel and air
 53 dynamic viscosity.

54 The advection equation for density (2) can be replaced by an advection equation for the
 55 concentration (6):

$$\partial_t c + \nabla \cdot (c\mathbf{u}) = \mathbf{0}. \quad (6)$$

56 Concerning the numerical approach to solve (1)–(3), a brief but accurate summary of the
 57 numerical discretization and schemes is provided at following paragraph. The fully detailed
 58 numerical approach can be found in [19, 20], where numerical and discretization schemes are
 59 explained. A second-order scheme is used for time discretisation at any given time-step n :

$$\rho_{n+\frac{1}{2}} \left(\frac{\mathbf{u}_{n+1} - \mathbf{u}_n}{\Delta t} + \mathbf{u}_{n+\frac{1}{2}} \cdot \nabla \mathbf{u}_{n+\frac{1}{2}} \right) = -\nabla p_{n+\frac{1}{2}} + \nabla \cdot (\mu_{n+\frac{1}{2}} (\mathbf{D}_n + \mathbf{D}_{n+1})) + (\sigma k \delta_s \mathbf{n})_{n+\frac{1}{2}}, \quad (7)$$

$$\frac{c_{n+\frac{1}{2}} - c_{n-\frac{1}{2}}}{\Delta t} + \nabla \cdot (c_n \mathbf{u}_n) = \mathbf{0}, \quad (8)$$

$$\nabla \cdot \mathbf{u}_n = \mathbf{0}. \quad (9)$$

62 The calculation of the velocity and the pressure field are decoupled through an intermediate
 63 velocity, \mathbf{u}_\star , using the Chorin's projection method [21]:

$$\mathbf{u}_{n+1} = \mathbf{u}_\star - \frac{\Delta t}{\rho_{n+\frac{1}{2}}} \nabla p_{n+\frac{1}{2}}, \quad (10)$$

64 and the system is simplified into the following expression

$$\rho_{n+\frac{1}{2}} \left(\frac{\mathbf{u}_\star - \mathbf{u}_n}{\Delta t} + \mathbf{u}_{n+\frac{1}{2}} \cdot \nabla \mathbf{u}_{n+\frac{1}{2}} \right) = +\nabla \cdot (\mu_{n+\frac{1}{2}} (\mathbf{D}_n + \mathbf{D}_\star)) + (\sigma k \delta_s \mathbf{n})_{n+\frac{1}{2}}, \quad (11)$$

$$\frac{c_{n+\frac{1}{2}} - c_{n-\frac{1}{2}}}{\Delta t} + \nabla \cdot (c_n \mathbf{u}_n) = \mathbf{0}, \quad (12)$$

$$\nabla \cdot \mathbf{u}_\star = \nabla \cdot \left(\frac{\Delta t}{\rho_{n+\frac{1}{2}}} \nabla p_{n+\frac{1}{2}} \right). \quad (13)$$

67 The advective term in Equation (11), $\mathbf{u}_{n+\frac{1}{2}} \cdot \nabla \mathbf{u}_{n+\frac{1}{2}}$ is computed using the Bell-Colella-Glaz
 68 second-order unsplit upwind scheme [22, 19], which is numerically stable for CFL numbers
 69 smaller than one. The advection equation (12) for the volume concentration is solved using a
 70 piecewise-linear geometrical Volume-of-Fluid (VOF) scheme [20].

71 The surface-tension term in Equation (11), $(\sigma k \delta_s \mathbf{n})_{n+\frac{1}{2}}$, is computed as described by Stéphane
 72 Popinet [20] combining a continuum-surface-force (CSF) approach and a height-function cur-
 73 vature estimation. This approach solves the known parasitic currents problem that are found
 74 classically in CSF when a stationary droplet in theoretical equilibrium is considered.

75 An important feature of the code is the octree mesh for 3D (or quad mesh in 2D) that allows
 76 adaptive refinement in each time-step. Three different criteria for the refinements have been
 77 used: in terms of vorticity to a proper characterization of the turbulence, in terms of gradient of
 78 concentration to accurately capture the interface and in terms of radius of curvature to describe
 79 the break-up process.

80 This code has been validated against linear instability theory [15] considering two-phase
 81 parallel mixing layers comparing the predicted temporal growth of small disturbances induced
 82 in the flow, obtaining a good agreement between numerical and theoretical results. The errors
 83 of the position of the maximum height of the wave were always below 5%. The ability of the
 84 code to simulate primary applications in jets at low velocity (20 m/s) has been also tested in
 85 that paper, as well as for the case of a hollow-cone atomizer with same velocity but adding swirl
 86 movement. The results were compared with experimental images, obtaining similar flow patterns
 87 experimentally and computationally.

88 Using low jet velocity, the code has been also used to predict the behaviour of impinging jets
 89 in [23]. In this paper, the authors compared the liquid sheet morphology for two identical liquid
 90 jets impinging at a given instant. They obtained numerical convergence and good agreement with
 91 experimental results based on measurements of droplet size. Finally, in [17], the code is used to
 92 simulate a spray of a diesel injector. Results obtained from the code were compared in terms of
 93 droplet radius with experiments from Hiroyasu and Kadota [24].

94 3. Mesh Sensivity

95 Concerning to the mesh, 3 parameters have been studied: cell size, domain width and maxi-
 96 mum number of cells.

97 3.1. Cell Size

98 As it is showed in Figure 1, a coarse mesh results in a lack of accuracy and unrealistic spray
 99 with big droplets and very low atomization. However, a finer mesh is able to accurately capture
 100 the physics of the spray at the expense of increasing the number of cells, and consequently the
 101 computational time.

102 In the computational study, several minimum cell sizes ranging from 24 μm to 1 μm (Table
 103 1) were studied. Something to highlight is that when the minimum cell size is divided by 2 the
 104 number of cells increase roughly by a factor of 8 (in the case of a uniform mesh they increase
 105 exactly by a factor of 8).

minimum cell sizes (μm)	1, 1.5, 2, 3, 4, 6, 8, 9, 12, 16, 24
--------------------------------------	--------------------------------------

Table 1: Minimum cell size cases

106 A mesh independence study involving different minimum cell sizes was performed to estab-
 107 lish the cell size requirements depending on the parameter of the spray to be analyzed. From
 108 this study two different requirements for the cell size have been achieved: for the study of an
 109 external property of the spray, such as the spray penetration, the convergence is achieved for a
 110 cell size of 9 μ , while for the study of an internal spray characteristic, such as the breakup length
 111 a minimum cell size of 2 μ is required. The study was performed by comparing the numerical
 112 results in terms of penetration or breakup length coming from different meshes (decreasing the

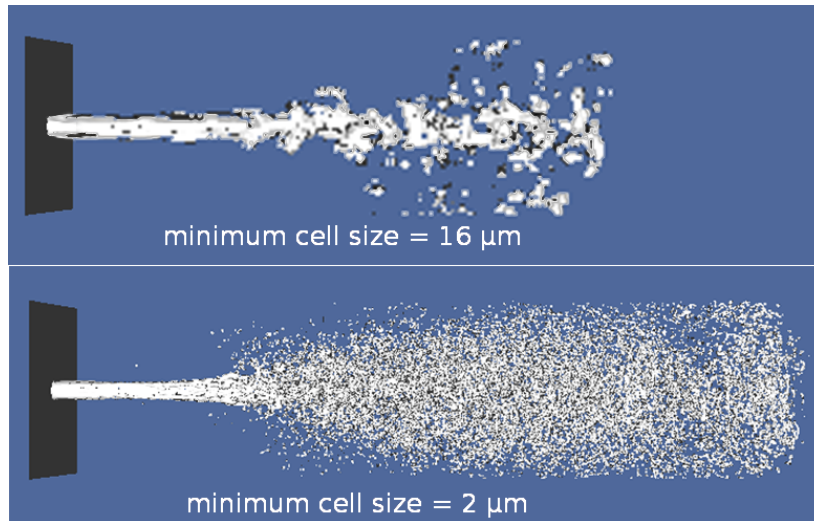


Figure 1: Minimum cell size

113 minimum cell size) in order to detect the convergence of results, and therefore the cell size which
 114 guarantees best results with low computational cost.

115 3.2. Domain Width

116 In Figure 2 the domain of the simulation is shown. This domain is characterized by the width,
 117 L and the length, which is five times the width. In the Figure the diameter of the orifice where
 118 the fuel is injected is represented by D_0 . Free stream boundaries have been set at the top and
 119 at the bottom of the domain. With the aim of reducing as much as possible the computational
 120 cost, small values of L/D_0 were initially tested, but important divergence problems arisen when
 121 the fuel droplets approached to the vicinity of the boundaries. In particular, the problem is pro-
 122 duced when a vorticity field placed around the spray tip, where velocity dramatically increases,
 123 approaches to the free stream boundaries.

124 In order to optimize the domain, three different L/D_0 ratios have been tested (5, 10 and 20).

125 Results are plotted in Figure 3. In the upper part, the simulation time is displayed versus the
 126 number of iterations. In the bottom of the Figure, the time-step is plotted against the same pa-
 127 rameter. As can be seen, for the smaller value ($L/D_0 = 5$), the time-step is dramatically reduced
 128 (from iteration 2000 on) and tends asymptotically to zero, resulting in the higher number of iter-
 129 ations required to make the simulation progress. Nevertheless, no significative differences were
 130 found in terms of time-step when comparing the cases of $L/D_0 = 10$ and $L/D_0 = 20$. In order to
 131 guarantee convergence and reduce the domain size as much as possible (less computational cost)
 132 a domain width orifice diameter ratio of 10 has been used.

133 3.3. Maximum Number of Cells

134 Due to the Adaptive Mesh Refinement (AMR) algorithm used, the number of cells drasti-
 135 cally increases along the simulation when the number of droplets increases due to the atomiza-
 136 tion process. In order to avoid an increase without limit and a saturation of the computational

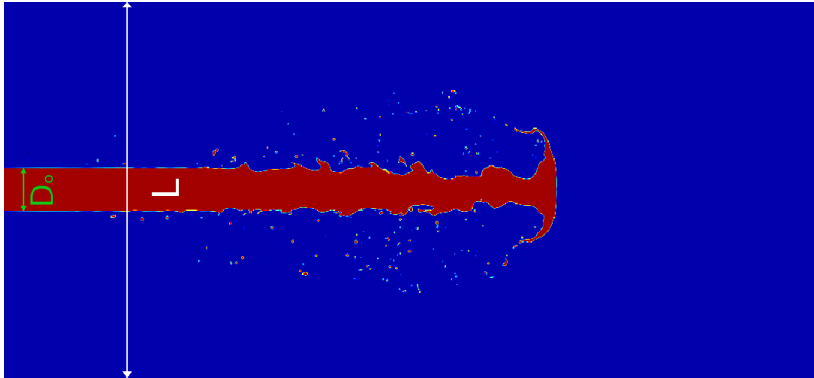


Figure 2: Domain width

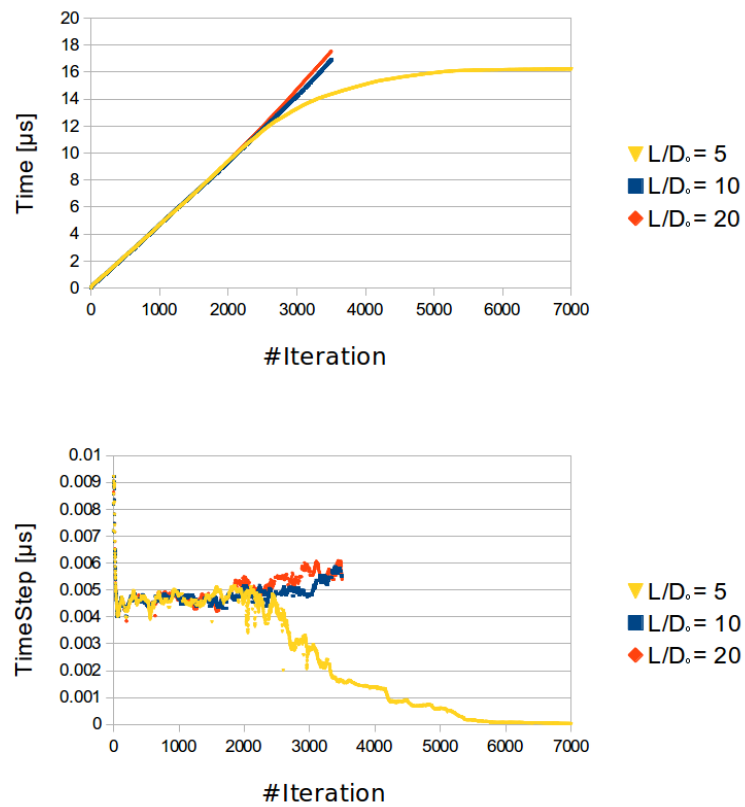


Figure 3: Domain width - orifice length ratios

137 resources (32 CPUs per simulation), the effect on the results of limiting the maximum number of
138 cells has been studied. As showed in Table 2, six different limits have been tested.

Maximum number of cells [-]	Maximum number of cells per CPU (32 CPUs) [-]
800k	25k
1.6M	50k
3.2M	100k
6.4M	200k
12.8M	400k

Table 2: Maximum number of cells

139 During the simulation, when the maximum number of cells is reached, cells are created or
140 removed according to AMR cost function criteria, suffering a redistribution but keeping the total
141 number. In Figure 4, the axial velocity of the spray is depicted versus the axial position for all
142 the tested maximum number of cells. The case of a simulation time of 10 μs is exhibited in the
143 upper part and the case of 18 μs in the bottom part. It can be noted that for 10 μs (upper part),
144 the spray tip penetration is around 2 mm and the maximum number of cells is not supposed to be
145 reached in any case, and so, all the plotted cases behave exactly in the same way. Nevertheless,
146 after 18 μs of simulation (bottom part), the spray tip penetration is around 3 mm , and due to the
147 spray development and atomization, the use of a limitation of 25k would lead to stability and
148 convergence problems.

149 In order to study the first 7-8 millimeters of the Diesel spray where primary atomization
150 takes place [8], the results of this study has proved that it is required to use the extreme case of
151 12.8 M cells as a maximum value (that is the same 400k cells per CPU) because with this value
152 convergence and stability problems are avoided even when the maximum number is reached.

153 4. Validation

154 The theoretical model from Desantes et al. [25] have been used for validation. It is a theo-
155 retical model for the non-perturbed zone length and the drop of velocity in the spray axis in the
156 main region of the spray. As it is drawn in Figure 5, the non-perturbed zone is the axial distance
157 from the orifice where there is only liquid in the axis (liquid core) and the axial velocity is equal
158 to the injection velocity and so, it is not perturbed by the entrained air. The main region is the
159 zone where the liquid core does not further exist because all the fluid has been atomized into
160 small droplets and the axial velocity decreases with the axial position [6, 7, 8].

161 This model has been extensively validated against measurements of axial velocity in the
162 spray axis obtained with a phase Doppler particle analyzer (PDPA) [7, 25] and also using X-ray
163 projected mass distribution measurements [8, 26] that were converted into fuel mass concentra-
164 tion in the axis. The relationship between axial velocity and axial mass concentration through
165 the Schmidt number [8, 26] allowed validating also this theoretical model with those complex
166 measurements.

167 The model is based in momentum flux conservation and considers local density variations
168 inside the spray and a generic Schmidt number. A complete model description and the assump-
169 tions under the model is derived are given in [26] where the following equation (14) that relates
170 the velocity in the axis with the axial position is obtained:

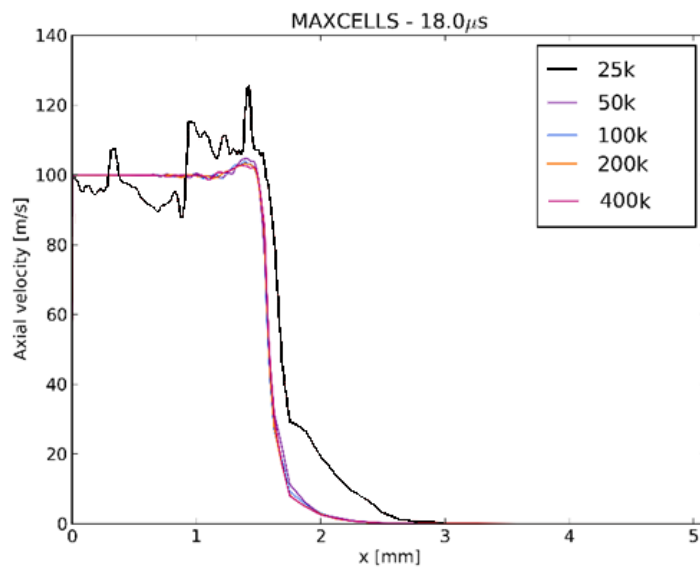
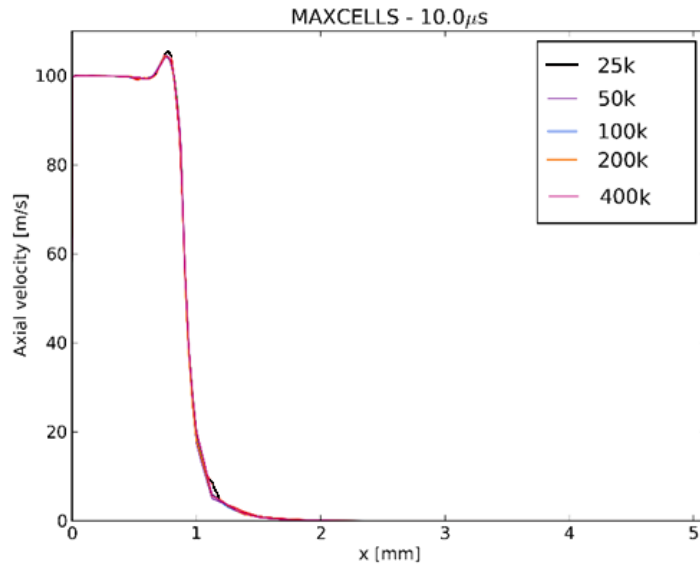


Figure 4: Maximum number of cells - divergence

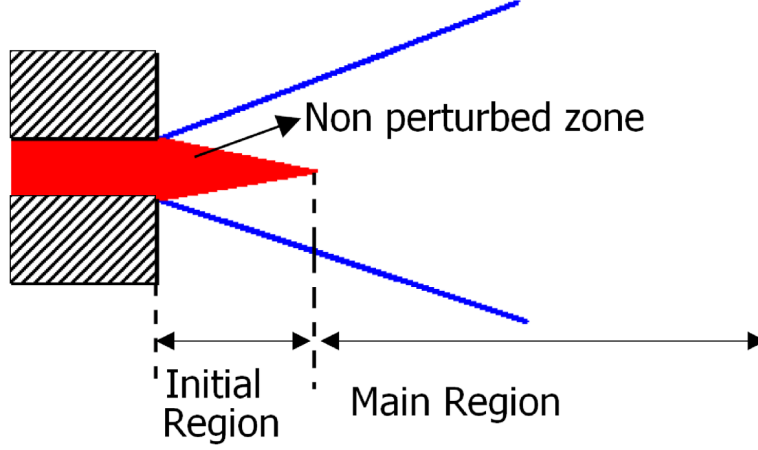


Figure 5: Spray zones

$$M_0 = \frac{\pi}{2\alpha} \rho_a \tan\left(\frac{\theta_u}{2}\right) x^2 U_{axis}^2 \sum_{i=0}^{\infty} \frac{2}{2+i \cdot Sc} \left[\left(\frac{U_{axis}}{U_0} \right) \left(\frac{1+Sc}{2} \right) \frac{\rho_f - \rho_a}{\rho_f} \right]^i, \quad (14)$$

171 where M_0 is the axial momentum flux, Sc is the Schmidt number, ρ_f is the density of the fuel, ρ_a
 172 is the density of the air, $U_{axis} = U_{axis}(x)$ is the velocity in the axis, α is the shape factor of the
 173 Gaussian profile representative of the radial component of the velocity inside the spray, and θ_u is
 174 the velocity spray cone angle.

175 A case with the physical characteristics of Table 3 has been set up and the outcomes have
 176 been compared in terms of velocity drop in the axis with the one expected by Equation (14). The
 177 comparison have been performed with 2 Schmidt numbers, $Sc = 0.6$, which was demonstrated
 178 in [26] to be inside a suitable Schmidt number range in diesel sprays [8, 26], and $Sc = 1$, which
 179 is normally used for spray modelers because it simplifies equation (14) [6]. A more scientific
 180 reason that justifies the use $Sc = 1$ is the fact that, although an optimal value of $Sc = 0.6$ could
 181 explain the axial velocity drop along the spray axis, the breakup length is better estimated with
 182 the 0D mathematical model when a value of $Sc = 1$ was used [26].

183 In Figure 6 the drop in the velocity along the axis of the spray is shown. Results coming
 184 from the theoretical model (with two values of Schmidt number) are compared to the results of
 185 the 3D simulation. For this last, the value of the spray angle was calculated by fitting the radial
 186 velocity profiles to Gaussian profiles following the same procedure described in [25]. From the
 187 results it can be observed a good agreement between the theoretical model and the simulation. It
 188 is worthy of mention that, as was the case in the comparison of the 0D model with experimental
 189 X-ray projected mass distribution measurements [8, 26], the results of the 3D simulation (in that
 190 case experimental values) are closer to the velocity decrease provided by the 0D model when a
 191 Schmidt number of 0.6 is used, and, what is more important, the simulation and the 0D model
 192 basically provide the same intact length with small deviation when the Schmidt number equals
 193 unity.

D_0	156 μm
ρ_f	843 kg/m^3
ρ_a	17 kg/m^3
μ_f	2.4e-3 Pa · s
μ_a	2.872e-5 Pa · s
U_0	100 m/s
σ	2.5e-2 N/m

Table 3: Physical characteristics for validation

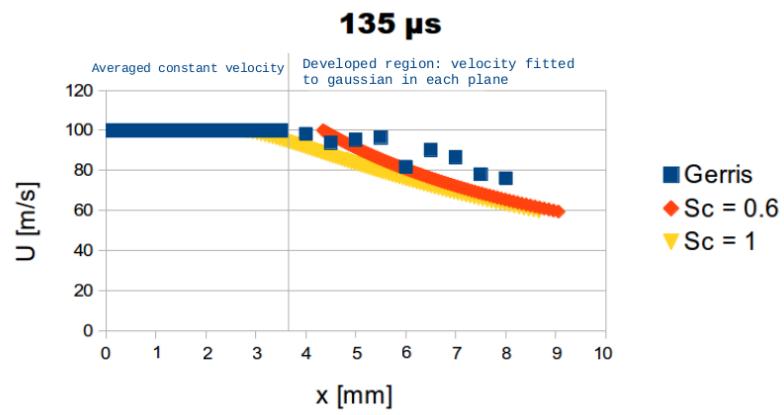


Figure 6: Axial velocity drop

194 **5. Influence of Periodic Velocity Perturbation**

195 After the validation, the influence of a periodic perturbation in the injection velocity (inlet
196 boundary condition) on the atomization process has been analysed. In order to achieve this
197 objective, a small sinusoidal perturbation in the inlet velocity given by equation (15) has been
198 considered for several frequencies, f :

$$U = U_0 (1 + 0.05 \sin(2\pi \cdot f \cdot t)). \quad (15)$$

199 This sinusoidal perturbation simulates the pressure oscillations that normally occur in actual
200 injection systems mainly due to the dynamic behavior of the injector.

201 The exterior non-perturbed length parameter, L_{np} , has been chosen in order to study the
202 influence of the perturbations on the spray morphology. As it is drawn at Figure 7, L_{np} is the
203 length measured from the orifice where there is not perturbation in the spray surface, so, there is
204 not atomization or it is negligible.

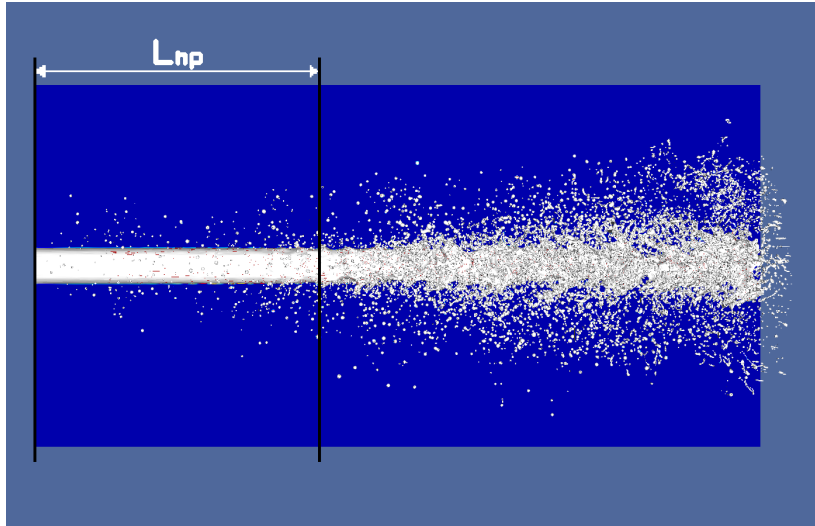


Figure 7: Exterior non-perturbed length

205 The physical characteristics of the fuel used to perform this study are showed at Table 4.

206 For this study, the frequency has been varied from 0.2 MHz to 2.2 MHz in steps of 0.2 MHz
207 and also a lowest frequency of 0.1 MHz has been tested. Outcomes have been drawn at Figure 8.
208 As can be observed the tendency of L_{np} over frequency has been captured in a good fit. Higher
209 frequency implies lower L_{np} and L_{np} tends asymptotically to zero as the frequency grows. This
210 result implies that pressure perturbation in the injection system that induce velocity fluctuations
211 could improve the atomization of the spray (diminution of L_{np}).

212 **6. Conclusions**

213 In this section, the main conclusions of the work presented in this paper are drawn:

D_0	100 μm
ρ_f	696 kg/m^3
ρ_a	25 kg/m^3
μ_f	1.2e-3 $\text{Pa} \cdot \text{s}$
μ_a	1.0e-5 $\text{Pa} \cdot \text{s}$
U_0	100 m/s
σ	6.0e-2 N/m

Table 4: Physical characteristics for periodic perturbation study

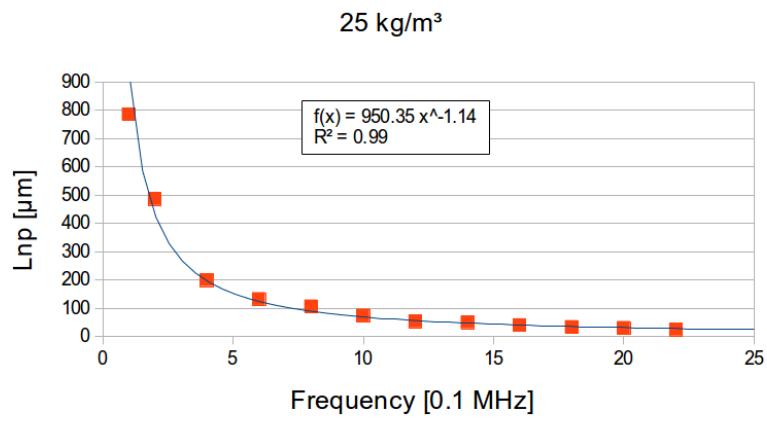


Figure 8: Exterior non-perturbed length over frequency

214 In this paper, a new multiphasic code for incompressible flow has been studied for using in
215 diesel spray simulations. The study has been performed using low injection velocity in order
216 to reduce the computational cost. First of all, a mesh sensitivity study has been performed over
217 the different possible parameters defining the mesh, namely, domain width, refinement levels
218 and limiting the maximum number of cells in the domain. From this first study the following
219 conclusions have been extracted:

- 220 • Two different refinement levels should be used depending on the objective:
 - 221 – For the study of external properties of the spray like the spray penetration, a cell size
222 of 9 micrometers has been found to guarantee convergence and reliable results.
 - 223 – For the study of inner properties such as droplet characteristics or liquid core length,
224 a cell size of 2 micrometers is required.
- 225 • In order to guarantee convergence and reduce the domain size as much as possible and
226 so, reducing the computational cost, a domain width-orifice diameter ratio, L/D of 10
227 has been obtained as an optimal value to study the first millimeters of the spray (about 8
228 millimeters).
- 229 • In order to study the first millimeters of a diesel spray (8 millimeters), a maximum number
230 of cells of 12.8M cells has been found to be enough to reduce convergence problems.

231 The code has been validated by comparing with a theoretical 0D model based on momentum
232 flux conservation in the spray. This 0D model has been extensively validated previously with
233 complex measurements using X-Rays. The validation has been made in terms of the velocity
234 evolution in the spray axis and liquid core length. The results of the simulations showed an
235 acceptable agreement of the model with the 0D model results in predicting the axial velocity and
236 the liquid core length.

237 Finally, the influence of periodic perturbation of the injection velocity on the spray atomiza-
238 tion has been studied. This perturbation simulates the pressure oscillations that normally occur
239 in the injection process of Diesel injection systems, which in turns, lead to injection velocity
240 oscillations. A sinusoidal function with amplitude variation of 5% and different frequencies has
241 been tested. The level of atomization has been characterized using the external non-perturbed
242 length (L_{np}) which is the length of the spray closer to the orifice where there is no perturbation
243 in the surface, and so, atomization does not take place.

244 From this final study, the following conclusions have been drawn:

- 245 • The non-perturbed length clearly depends on the frequency: the higher the frequency of
246 the perturbation, the lower the non-perturbed length. An exponential function has been
247 found to fit the results with high level of reliability ($R^2 = 0.99$).
- 248 • From this finding, it can be conclude that oscillations in the injection velocity enhance the
249 atomization process.

250 Acknowledgements

251 This work was sponsored by “Ministerio de Economía y Competitividad” of the Spanish
252 Government in the frame of the Project “Comprensión de la influencia de combustibles no con-
253 convencionales en el proceso de inyección y combustión tipo diesel”, Reference TRA2012-36932 and

254 MTM2913-41765-P. Additionally, the hardware used for the project was purchased with fund-
255 ing from Ministerio de economía y competitividad FEDER-ICTS-2012-06. The authors would
256 also like to thank the computer resources, technical expertise and assistance provided by the
257 Universitat de València in the use of the supercomputer “Tirant”.

258 **Nomenclature**

259 c : concentration
260 \mathbf{D} : deformation tensor
261 D_0 : orifice diameter
262 f : frequency
263 k : curvature
264 L : domain width
265 M : momentum flux
266 \mathbf{n} : normal vector
267 p : pressure
268 Sc : Schmidt number
269 \mathbf{u} : velocity
270 **Greek symbols:**
271 α shape factor
272 δ_s Dirac distribution
273 θ_u velocity spray angle
274 μ dynamic viscosity
275 ρ density
276 σ surface tension coefficient
277 **Subscripts:**
278 f: fuel
279 a: air

280 **Conflict of Interest Statement**

281 The authors declare that there is no conflict of interests regarding the publication of this
282 article.

283 **References**

- 284 [1] F. Payri, V. Bermúdez, F. J. Salvador, The influence of cavitation on the internal flow and the spray characteristics
285 in diesel injection nozzles, *Fuel* 83 (2004) 419–431.
286 [2] R. Payri, F. J. Salvador, J. Gimeno, V. Soare, Determination of Diesel sprays characteristics in real engine in-
287 cylinder air density and pressure conditions, *Journal of mechanical science and technology* 19 (11) (2005) 2040–
288 2052.
289 [3] V. Bermúdez, R. Payri, F. J. Salvador, A. H. Plazas, Study of the influence of nozzle seat type on injection rate and
290 spray behaviour, *Proceedings of the Institution of Mechanical Engineers, Part D: Journal of Automobile Engineer-*
291 *ing* 219 (5) (2005) 677–689.
292 [4] F. J. Salvador, S. Ruiz, J. M. Salaver, J. De la Morena, Consequences of using biodiesel on the injection and airfuel
293 mixing processes in diesel engines, *Proceedings of the Institution of Mechanical Engineers, Part D: Journal of*
294 *Automobile Engineering* 227 (8) (2012) 1130–1141.
295 [5] R. Payri, F. J. Salvador, J. Gimeno, J. De la Morena, Influence of injector technology on injection and combustion
296 development Part 2: Combustion analysis, *Applied Energy* 88 (4) (2011) 11301139.

- 297 [6] J. M. Desantes, R. Payri, F. J. Salvador, A. Gil, Development and validation of a theoretical model for diesel spray
298 penetration, *Fuel* 85 (7-8) (2006) 910917.
- 299 [7] R. Payri, B. Tormos, F. J. Salvador, L. Araneo, Spray droplet velocity characterization for convergent nozzles with
300 three different diameters, *Fuel* 87 (15-16) (2008) 31763182.
- 301 [8] J. M. Desantes, F. J. Salvador, J. J. López, J. De la Morena, Study of mass and momentum transfer in diesel sprays
302 based on X-ray mass distribution measurements and on a theoretical derivation, *Experiments in Fluids* 50 (2) (2011)
303 233–246.
- 304 [9] F. J. Salvador, S. Hoyas, R. Novella, J. Martínez-López, Numerical simulation and extended validation of two-
305 phase compressible flow in diesel injector nozzles, *Proceedings of the Institution of Mechanical Engineers, Part D:
306 Journal of Automobile Engineering* 225 (D4) (2011) 545–563.
- 307 [10] F. J. Salvador, J.-V. Romero, M.-D. Roselló, J. Martínez-López, Validation of a code for modeling cavitation
308 phenomena in Diesel injector nozzles, *Mathematical and Computer Modelling* 52 (7-8) (2010) 1123–1132.
- 309 [11] J. Revéillon, L. Vervisch, Spray vaporization in nonpremixed turbulent combustion modeling: a single droplet
310 model, *Combustion and Flame* 121 (1-2) (2000) 75–90.
- 311 [12] F. J. Salvador, J. Gimeno, J. M. Pastor, P. Martí-Aldaraví, Effect of turbulence model and inlet boundary condition
312 on the diesel spray behavior simulated by an eulerian spray atomization (ESA) model, *International Journal of
313 Multiphase Flow* 65 (2014) 108–116.
- 314 [13] Y. Pan, K. Suga, Large eddy simulation of turbulent liquid jets into air, 2006, ICLASS Paper ICLASS06-219.
- 315 [14] F. J. Salvador, J. Martínez-López, J. V. Romero, M. D. Roselló, Computational study of the cavitation phenomenon
316 and its interaction with the turbulence developed in diesel injector nozzles by Large Eddy Simulation (LES), *Math-
317 ematical and Computer Modelling* 57 (7-8) (2013) 1656–1662.
- 318 [15] D. Fuster, A. Bagué, T. Boeck, L. Le Moyne, A. Leboissetier, S. Popinet, P. Ray, R. Scardovelli, S. Zaleski,
319 Simulation of primary atomization with an octree adaptive mesh refinement and VOF method, *International Journal
320 of Multiphase Flow* 35 (6) (2009) 550–565.
- 321 [16] T. Ménard, S. Tanguy, A. Berlemont, Coupling level set/VOF/ghost fluid methods: validation and application to 3D
322 simulation of the primary break-up of a liquid jet, *International Journal of Multiphase Flow* 33 (5) (2007) 510–524.
- 323 [17] K. Mehravaran, Direct simulations of primary atomization in moderate speed diesel fuel injection, *International
324 Journal of Materials, Mechanics and Manufacturing* 1 (2) (2013) 207–209.
- 325 [18] F. Dos Santos, L. Le Moyne, Spray atomization models in engine applications, from correlations to direct numerical
326 simulations, *Oil and Gas Science and Technology* 66 (5) (2011) 801–822.
- 327 [19] S. Popinet, Gerris: A tree-based adaptive solver for the incompressible Euler equations in complex geometries,
328 *Journal of Computational Physics* 190 (2) (2003) 572–600.
- 329 [20] S. Popinet, An accurate adaptive solver for surface-tension-driven interfacial flows, *Journal of Computational
330 Physics* 228 (16) (2009) 5838–5866.
- 331 [21] A. Chorin, On the convergence of discrete approximation to the Navier-Stokes equations, *Mathematics of Compu-
332 tation* 23 (1969) 341–353.
- 333 [22] J. Bell, H. Colella, H. Glaz, A second-order projection method for the incompressible Navier-Stokes equations,
334 *Journal of Computational Physics* 85 (1989) 257–283.
- 335 [23] X. Chen, D. Ma, V. Yang, S. Popinet, High-fidelity simulations of impinging jet atomization, *Atomization and
336 Sprays* 23 (12) (2013) 1079–1101.
- 337 [24] H. Hiroyasu, T. Kadota, Fuel droplet size distribution in diesel combustion chamber, SAE Technical PapersSAE
338 Paper 740715.
- 339 [25] J. M. Desantes, R. Payri, J. M. García, F. J. Salvador, A contribution to the understanding of isothermal diesel spray
340 dynamics, *Fuel* 86 (7-8) (2007) 1093–1101.
- 341 [26] F. J. Salvador, S. Ruiz, J. Gimeno, J. De la Morena, Estimation of a suitable Schmidt number range in diesel sprays
342 at high injection pressure, *International Journal of Thermal Sciences* 50 (2011) 1790–1798.